

Efficient ion acceleration and dense electron-positron plasma creation in ultra-high intensity laser-solid interactions

D. Del Sorbo,¹ D. R. Blackman,¹ R. Capdessus,² K. Small,¹ C. Slade-Lowther,¹ W. Luo,² M. J. Duff,² A. P. L. Robinson,³ P. McKenna,² Z.-M. Sheng,² J. Pasley,¹ and C. P. Ridgers¹

¹*York Plasma Institute, Physics Department, University of York, York YO10 5DQ, United Kingdom*

²*Department of Physics SUPA, University of Strathclyde, Glasgow G4 0NG, United Kingdom*

³*Central Laser Facility, STFC Rutherford-Appleton Laboratory, Oxfordshire OX11 0QX, United Kingdom*

The radiation pressure of next generation ultra-high intensity ($> 10^{23}$ W/cm²) lasers could efficiently accelerate ions to GeV energies. However, nonlinear quantum-electrodynamic effects play an important role in the interaction of these laser pulses with matter. Here we show that these effects may lead to the production of an extremely dense ($\sim 10^{24}$ cm⁻³) pair-plasma which absorbs the laser pulse consequently reducing the accelerated ion energy and energy conversion efficiency by up to 30-50% & 50-65%, respectively. Thus we identify the regimes of laser-matter interaction where either ions are efficiently accelerated or dense pair-plasmas are produced as a guide for future experiments.

Ultra-high intensity lasers accelerate ions over much shorter distances than conventional accelerators (microns compared to many meters) with potential applications in medical physics [1] (hadron therapy) as well as in fundamental physics [2] (hadron interactions). Next generation lasers, such as those comprising the soon to be completed Extreme Light Infrastructure [3], could accelerate ions to GeV energies [4, 5]. However, at the intensities expected to be reached in these laser-matter interactions ($I > 10^{23}$ W/cm²), the laser very rapidly ionizes the target to form a plasma in which nonlinear quantum-electrodynamic (QED) effects play a crucial role [6]. Energetic electrons radiate gamma-ray photons by nonlinear Compton scattering. The radiated gamma-ray photons can generate electron-positron pairs in the laser-fields [7] which can radiate further photons. A cascade of pair production ensues, similar to that thought to occur in extreme astrophysical environments such as pulsar [8] and black hole [9] magnetospheres. Pair-plasmas more than eight orders of magnitude denser than currently achievable with ultra-high intensity lasers could be produced [10, 11], enabling the study of collective behavior in relativistic pair-plasmas.

At intensities soon to be reached ($I > 10^{22}$ W/cm²), the radiation pressure ion acceleration mechanism dominates [12] (with a more favorable scaling of ion energy with laser intensity $\epsilon \propto I$ compared to current experiments in the target normal sheath acceleration regime $\epsilon \propto \sqrt{I}$ [13–16]). In this acceleration scheme, the electromagnetic momentum carried by the laser pushes forwards the electrons at the front of the target, leaving a charge separation layer and creating an electrostatic field that in turn acts on the ions and leads to their acceleration. There are two regimes of radiation pressure ion acceleration depending on whether the target is thicker or thinner than the relativistic skin depth $\delta_s = c/(\sqrt{\gamma_e}\omega_{pe})$, where γ_e is the average Lorentz factor of electrons in the plasma and c the speed of light. $\omega_{pe} = \sqrt{4\pi n_e e^2/m_e}$ is

the electron plasma frequency (n_e is the electron density, e is the elementary charge and m_e is the electron mass). The case where the target is thicker than δ_s is known as hole boring (HB), because the intense radiation pressure of the laser punches a hole in the target, snowploughing ions forwards at an approximately constant speed [17, 18]. The case where the target thickness is $\ell \leq \delta_s$ is known as the light sail (LS) acceleration [19]. Here the target is sufficiently thin that the ions do not need to snowplough through the undisturbed target and so continuously accelerate [5]. Experiments have been performed in both regimes indicating the expected scaling of ion energy with laser intensity (although complicated by electron heating and the break up of very thin targets) [12, 20–27].

In this letter we use 3D particle-in-cell (PIC) simulations to demonstrate that QED effects can reduce the energy of radiation pressure accelerated ions by up to 50%. We show that the key role is played by an electron-positron plasma, created by a pair cascade between the laser and the target. This pair-plasma can reach the relativistically corrected critical density $n_c^{rel} = \gamma_e n_c = \gamma_e m_e \omega_{pe}^2 / (4\pi e^2)$, i.e. the density at which its dynamics will strongly affect the propagation of the laser pulse [28, 29]. In fact this pair-plasma may absorb the laser pulse [30, 31]. Consequently, the energy of the accelerated ions is strongly reduced. Depending on the laser intensity and target density, we identify two regimes of next generation laser-plasma interactions: a regime where laser energy is efficiently converted to pairs and gamma-rays and consequently the opposite regime where laser energy is efficiently converted to ion energy. The identification of the different regimes of ultra-high intensity laser-solid interaction will be crucial to the choice of parameters for experiments aiming at either ion acceleration or pair-plasma creation.

Simulations are performed with the particle-in-cell (PIC) code EPOCH [32], which includes both plasma

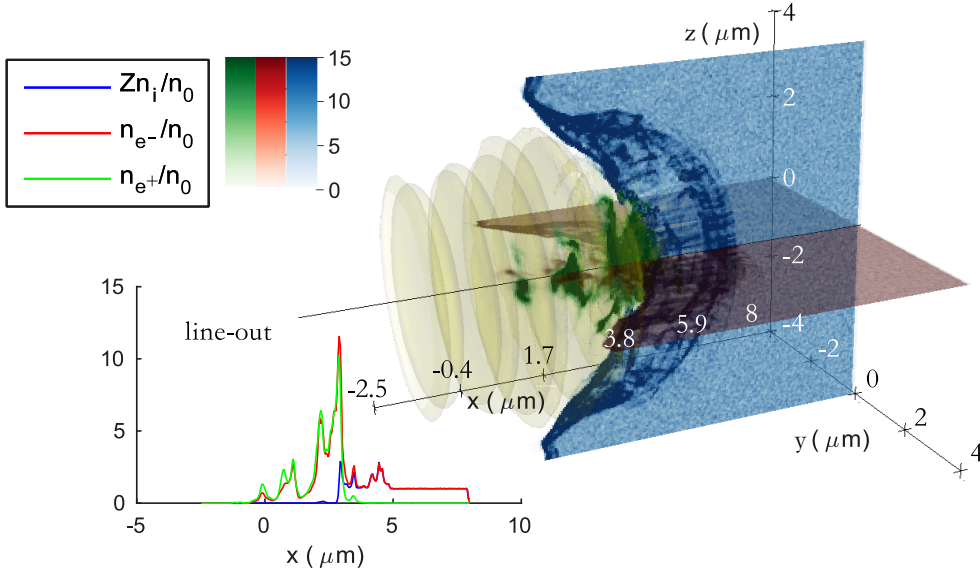


FIG. 1. QED HB acceleration at $t = 6T_L$. The laser is shown in yellow while the 3D target is shown as 2D slices of ions Zn_i/n_0 (blue), electrons n_{e-}/n_0 (red) and positrons n_{e+}/n_0 (green), with Z as the ionization number. Line-outs of particle densities at $y=z=0 \mu\text{m}$ are also present. They are computed averaging over 12×12 cells.

physics and nonlinear QED interactions [33, 34], the latter according to Ref. [35]. Figure 1 shows 3D simulation results of HB ion acceleration in the regime where QED effects are important, at time $t = 6T_L$ (where $T_L \approx 3.33$ fs is the laser period). In this simulation the target is initialized as a $10 \mu\text{m} \times 8 \mu\text{m} \times 8 \mu\text{m}$ aluminum slab with front surface in the plane $x = 0$ and initial electron density $n_0 = 10^{24} \text{ cm}^{-3}$ represented by 1.44×10^9 macroions and 1.6×10^8 macroelectrons. It is illuminated by a circularly polarized $1 \mu\text{m}$ wavelength laser of intensity $5 \times 10^{24} \text{ W/cm}^2$. The laser spot spatial profile is a fifth-order supergaussian with $3.3 \mu\text{m}$ full width half maximum and a constant temporal profile, with duration 30 fs. The simulation is performed with $250 \times 200 \times 200$ spatial cells corresponding to spatial dimensions of $10.5 \mu\text{m} \times 8 \mu\text{m} \times 8 \mu\text{m}$.

The simulation can be summarized as follows: for $t < 3.4T_L$, QED effects do not play a significant role in the ion acceleration. As the simulation proceeds, a pair cascade develops, with the number of pairs initially growing exponentially. After $t \approx 3.4T_L$, the pair cascade results in the production of an electron-positron pair-plasma with density equal to the relativistically corrected critical density. This pair-plasma grows between the laser and the aluminum ions, forming a pair cushion similar to that described in Ref. [36]. This pair cushion absorbs the laser, reducing the energy of the accelerated ions and the efficiency of the acceleration. By modifying the absorption, the pair-plasma generated in front of the target reduces both the average ion energy and the efficiency of conversion of laser energy to ion energy. We can determine the energy reduction by analyzing the ratio between the average ion energy in the simulation described above

to that in the equivalent simulation where the QED effects are artificially switched off. At $t = 6T_L$ this ratio is ≈ 0.67 . The equivalent ratio comparing the efficiency of the ion acceleration, i.e. the total amount of energy coupled to the ions, is ≈ 0.5 .

We will now determine the laser intensities and target densities at which QED effects quench HB ion acceleration by deriving a simple one dimensional model for circularly polarized lasers [12]. We assume that the HB proceeds at quasi-constant speed, i.e. ions instantaneously neutralize the charge separation due to electron movement at each time step. In the reference frame of the piston (the HB frame), $\langle p_x \rangle \approx 0$ [37] (\vec{p} is the electron momentum and x as the incident laser direction) due to rapid force balance between the $\vec{v} \times \vec{B}$ force from the laser and the electrostatic force from charge separation. Thus, gamma-ray photons are emitted transversely to the plasma surface and their contribution can be omitted in the HB frame longitudinal momentum balance, $I'/c(1 + R') = 2\gamma_{HB}^2 \rho c^2 \beta_{HB}^2$, where $I' = (1 - \beta_{HB})/(1 + \beta_{HB}) I$ is the laser intensity, R' is the reflection coefficient, ρ is the initial target mass density, $\beta_{HB} = v_{HB}/c$ and γ_{HB} , respectively, the normalized speed and the Lorentz factor of the front surface of the target, i.e. of the HB frame. The primed quantities are computed in the HB frame, while, when omitted, quantities are computed in the laboratory frame.

From the HB frame longitudinal momentum balance, the ion energy in the laboratory frame is [12, 17, 38]

$$\epsilon = m_i c^2 \frac{2\Pi}{1 + 2\sqrt{\Pi}}, \quad \Pi = \frac{(1 + R')}{2} \frac{I}{\rho c^3}. \quad (1)$$

The efficiency of laser conversion into ion energy is given

by the ratio between accelerated ion energy per unit of surface and the laser energy per unit of surface, i.e. $\phi = \epsilon Z n_0 v_{HB} \tau_{HB} / (I \tau_P)$, where τ_P is the laser pulse duration and $\tau_{HB} = c \tau_L / (c - v_{HB})$ is the interval between when the pulse first strikes the slab and when the trailing edge of the pulse strikes the HB surface. Therefore,

$$\phi = \frac{2\sqrt{\Pi}}{1 + 2\sqrt{\Pi}} \frac{1 + R'}{2}. \quad (2)$$

QED radiation losses can cause almost complete laser absorption, i.e. $A' \approx 1$ and $R' \approx 0$. In this case, for strong radiation pressure ion acceleration ($\Pi \gg 1$), Eqs. (1) & (2) show that the ion energy is reduced by a maximum of $\sqrt{2}$ and the efficiency of ion acceleration by a maximum of 2; for weak acceleration ($\Pi \ll 1$), i.e. when ions are non-relativistic (although electrons remains ultrarelativistic), the ion energy and efficiency of acceleration are reduced by factors of 2 and $2\sqrt{2}$ respectively, consistently with a similar analysis, limited to the classical radiation reaction force [39].

The scaling laws given in Eqs. (1) and (2) require a prediction for the laser absorption caused by QED radiation losses. Several scaling laws for QED-mediated laser absorption have been discussed in the literature [40], for linear [41, 42] and circular [4, 43] laser polarization. In the simulation discussed above (and those discussed later) the laser absorption occurs almost entirely in the self-generated pair plasma. Therefore, QED effects only start to cause significant laser absorption when the density of the pair-plasma generated at the front surface of the target also approaches the relativistically corrected critical density. This occurs at a time we define as the absorption time t_a . As in Ref. [31], we assume that the absorption in the HB frame is negligible for $\tau_P < t_a$ and is $A'_{HB} = (1 - \frac{t_a}{\tau_P})$, for $\tau_P > t_a$.

It can be shown that, in the laboratory frame, the time required for the pair-plasma to reach the relativistically corrected critical density is $t_a = \gamma_{HB} \ln[2\gamma_e n_c / (\gamma_{HB} n_0) + 1] / \Gamma$, with the electron Lorentz factor γ_e and the QED parameter η (the electric field strength in the electron's rest frame relative to the critical field of QED $E_{crit} = 4.36$ G [44]) assumed constant in time and computed as described in Eq. (6) of Ref. [45], accounting for the Gaunt factor associated with QED photon emission. Γ is the rate of the exponential density growth as given in Eq. (10) of Ref. [30]. In addition we account for the fact that the field inside the target is reduced due to the skin effect in the relativistically overcritical plasma by correcting the intensity as follows: $I_{SD} = I \gamma_e n_c / (\gamma_{HB} n_0)$ [37].

The derived expression for t_a gives a model which uniquely determines the laser absorption, ion energy and efficiency of ion acceleration for a given laser intensity and target density. By iteratively solving the model, we can perform a systematic quantitative analysis of QED effects on HB. We limit the simulations used to verify the model to 1D and we chose aluminum targets for

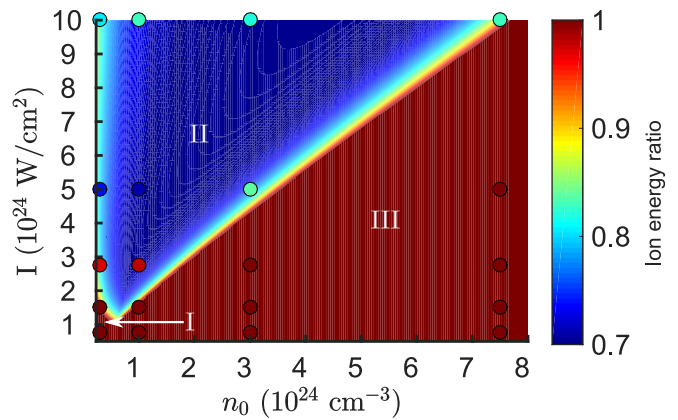


FIG. 2. Ratio of QED to classical ion energy, as a function of both laser intensity ($5 \times 10^{23} \text{ W/cm}^2 \leq I \leq 10^{25} \text{ W/cm}^2$) and initial electron density ($2.3 \times 10^{23} \text{ cm}^{-3} \leq n_0 \leq 8 \times 10^{24} \text{ cm}^{-3}$). Dots represent simulation results, while the color-plot in the background represents the analytical model. Three regimes are identified: (I) relativistically underdense plasma, (II) QED-plasma regime and (III) relativistically overcritical plasma.

which QED effects are maximized, according to Eq. (1) ($\Pi \ll 1$). 10240 cells were used to discretize a domain of $20 \mu\text{m}$, initialized with 1.31072×10^6 macroelectrons and macroions per cell. In Fig. 2 we plot the ratio of the average ion energy including QED effects (i.e. laser absorption in the pair-plasma) to that neglecting QED effects, as a function of the initial electron density and of the laser intensity. The color scale gives the prediction of the model defined above, for a circularly polarized $1 \mu\text{m}$ wavelength laser pulse with $\tau_P = t = 30$ fs. We can identify three distinct regimes. Regime I: here the absorption is negligible and the acceleration can be explained using a classical HB model. This is because the initial target density is too low to initiate a pair cascade (given the probability of pair creation at that laser intensity). Regime II: as the density increases then a pair cascade can be initiated, resulting in the generation of a critical density pair-plasma and the quenching of ion acceleration. Regime III: if the initial target density is too high then the skin effect screens the laser fields and the cascade does not occur. In regimes I and III laser energy is efficiently (up to 100%) coupled to ion energy. In regime II laser energy is efficiently (up to 50%) coupled to electron-positron pairs and gamma-ray photons and a critical density pair-plasma is generated.

Figure 2 also shows 1D simulation results as colored dots for comparison to the model. The simulations show the same regimes as those predicted by the model.

The model developed here predicts temporal dependence of the average ion energy; the energy should begin to decrease after t_a . Figure 3 shows that this behavior is indeed seen in the simulations. Here we compare the tem-

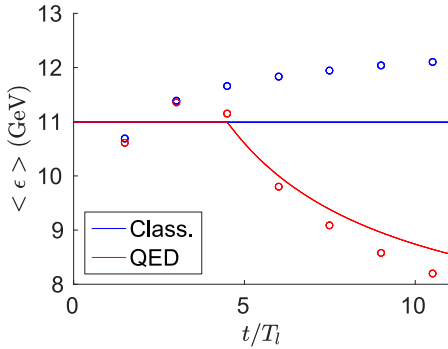


FIG. 3. Average ion energy as a function of time, for classical and QED simulations of a HB acceleration. Dots refers to simulation results while lines to theoretical predictions, assuming $t_a = 15$ fs.

poral dependence of the ion energy to the model prediction in the 1D simulation with the same physical parameters as the 3D simulation performed above. We see that after the absorption time $t_a \approx 4.5T_L \approx 15$ fs QED effects cause the ion energy to decrease. Also shown is the model prediction (where the absorption time from the simulation has been used to compute the ion energy reduction). In developing the model, we assumed that photons are emitted parallel to the target surface in the HB frame. This is consistent with the angle of photon emission seen in the simulations $\theta = \arccos(\langle p_x \rangle / \langle |\vec{p}| \rangle) \approx 47^\circ$ – on transformation to the laboratory frame the angle should be $\theta \approx \arccos(\beta_{HB})$ [37] which gives $\theta \approx 46^\circ$ for an average ion energy $\langle \epsilon \rangle \sim 10$ GeV.

Another target-parameter which can be varied is the thickness. By decreasing it, we can enter the LS scenario of radiation pressure ion acceleration. LS ion acceleration is particularly efficient [5]: accelerated targets can easily reach the ultrarelativistic limit ($\beta_{LS} \approx 1$). For this reason, the QED parameter $\eta \propto \sqrt{1 - \beta_{LS}^2}$ [45] is strongly reduced and consequently so are QED effects when compared to the HB cases considered above. This is supported by 1D simulations similar to those described above, but with the target thickness set by the condition for optimal LS ($\ell = a_0 n_c^{rel} / n_0 \lambda_L / \pi$ where λ_L is the laser wavelength [19]). In these simulations the target was accelerated much more efficiently than in the equivalent HB simulations (for $I \approx 5 \times 10^{24}$ W/cm² and $n_0 \approx 10^{24}$ cm⁻³ we found $\beta_{LS} \approx 1$ as compared to $\beta_{HB} \approx 0.7$). As predicted, in simulations of LS ion acceleration QED effects were indeed negligible for all laser intensities considered here, for example no absorption was seen for the LS simulation with $I \sim 10^{24}$ W/cm² compared to 70% for the equivalent HB simulation.

In conclusion, QED effects, specifically the creation of a critical density pair-plasma in front of the target, can quench HB radiation pressure ion acceleration, strongly reducing both the average ion energy (by up to 50%)

and the efficiency of conversion of laser energy to ion energy (by up to 65%). We have developed a practical model in order to estimate these reductions. This model demonstrates the regime where laser energy is efficiently converted to pairs and gamma-rays but also the regimes where this is not the case and laser energy is efficiently converted to ion energy. We have also found that QED effects do not affect LS ion acceleration. These observations will be useful for the design of experiments as they inform the choice of laser and target parameters depending on whether the generation of energetic ion beams or critical density pair-plasmas is the desired aim. Consequently, identifying these regimes of laser plasma interaction is crucial to the application of next generation lasers as a source of high energy ions, to enable the investigate antimatter and pair-plasmas at macroscopic scale, and to produce a very bright source of gamma-rays.

This work was funded by the UK Engineering and Physical Sciences Research Council (EP/K504178/1, EP/M018091/1, EP/M018156/1, EP/M018555/1 and EP/P007082/1). Computing resources have been provided by STFC Scientific Computing Department's SCARF cluster.

-
- [1] J. Caron, J.-L. Feugeas, B. Dubroca, G. Kantor, C. Dejean, G. Birindelli, T. Pichard, P. Nicolai, E. d'Humières, M. Frank, *et al.*, *Physica Medica* **31**, 912 (2015).
 - [2] S. Catani and M. Grazzini, *Phys. Rev. Lett.* **98**, 222002 (2007).
 - [3] G. Korn, B. LeGarrec, and B. Rus, in *CLEO: Science and Innovations* (Optical Society of America, 2013) pp. CTu2D-7.
 - [4] R. Capdessus and P. McKenna, *Physical Review E* **91**, 053105 (2015).
 - [5] T. Esirkepov, M. Borghesi, S. Bulanov, G. Mourou, and T. Tajima, *Phys. Rev. Lett.* **92**, 175003 (2004).
 - [6] A. Bell and J. G. Kirk, *Phys. Rev. Lett.* **101**, 200403 (2008).
 - [7] G. Breit and J. A. Wheeler, *Phys. Rev.* **46**, 1087 (1934).
 - [8] P. Goldreich and W. H. Julian, *The Astrophysical Journal* **157**, 869 (1969).
 - [9] R. D. Blandford and R. L. Znajek, *Monthly Notices of the Royal Astronomical Society* **179**, 433 (1977).
 - [10] H. Chen, S. C. Wilks, J. D. Bonlie, E. P. Liang, J. Myatt, D. F. Price, D. D. Meyerhofer, and P. Beiersdorfer, *Phys. Rev. Lett.* **102**, 105001 (2009).
 - [11] G. Sarri, K. Poder, J. Cole, W. Schumaker, A. Di Piazza, B. Reville, T. Dzelzainis, D. Doria, L. Gizzi, G. Grittani, *et al.*, *Nature communications* **6** (2015).
 - [12] A. Macchi, M. Borghesi, and M. Passoni, *Reviews of Modern Physics* **85**, 751 (2013).
 - [13] E. L. Clark, K. Krushelnick, J. R. Davies, M. Zepf, M. Tatarakis, F. N. Beg, A. Machacek, P. A. Norreys, M. I. K. Santala, I. Watts, and A. E. Dangor, *Phys. Rev. Lett.* **84**, 670 (2000).
 - [14] A. Maksimchuk, S. Gu, K. Flippo, D. Umstadter, and V. Y. Bychenkov, *Phys. Rev. Lett.* **84**, 4108 (2000).

- [15] R. A. Snavely, M. H. Key, S. P. Hatchett, T. E. Cowan, M. Roth, T. W. Phillips, M. A. Stoyer, E. A. Henry, T. C. Sangster, M. S. Singh, S. C. Wilks, A. MacKinnon, A. Offenberger, D. M. Pennington, K. Yasuike, A. B. Langdon, B. F. Lasinski, J. Johnson, M. D. Perry, and E. M. Campbell, *Phys. Rev. Lett.* **85**, 2945 (2000).
- [16] S. Wilks, A. Langdon, T. Cowan, M. Roth, M. Singh, S. Hatchett, M. Key, D. Pennington, A. MacKinnon, and R. Snavely, *Phys. Plasmas* **8**, 542 (2001).
- [17] A. Robinson, P. Gibbon, M. Zepf, S. Kar, R. Evans, and C. Bellei, *Plasma Physics and Controlled Fusion* **51**, 024004 (2009).
- [18] S. Weng, M. Murakami, P. Mulser, and Z. Sheng, *New Journal of Physics* **14**, 063026 (2012).
- [19] A. Macchi, S. Veghini, and F. Pegoraro, *Phys. Rev. Lett.* **103**, 085003 (2009).
- [20] C. A. J. Palmer, N. P. Dover, I. Pogorelsky, M. Babzien, G. I. Dudnikova, M. Ispiriyan, M. N. Polyanskiy, J. Schreiber, P. Shkolnikov, V. Yakimenko, and Z. Najmudin, *Phys. Rev. Lett.* **106**, 014801 (2011).
- [21] J. Badziak, S. Glowacz, S. Jablonski, P. Parys, J. Wolowski, and H. Hora, *Applied physics Lett.* **85**, 3041 (2004).
- [22] K. U. Akli, S. B. Hansen, A. J. Kemp, R. R. Freeman, F. N. Beg, D. C. Clark, S. D. Chen, D. Hey, S. P. Hatchett, K. Highbarger, E. Giraldez, J. S. Green, G. Gregori, K. L. Lancaster, T. Ma, A. J. MacKinnon, P. Norreys, N. Patel, J. Pasley, C. Shearer, R. B. Stephens, C. Stoeckl, M. Storm, W. Theobald, L. D. Van Woerkom, R. Weber, and M. H. Key, *Phys. Rev. Lett.* **100**, 165002 (2008).
- [23] A. Henig, D. Kiefer, M. Geissler, S. G. Rykovanov, R. Ramis, R. Hörlein, J. Osterhoff, Z. Major, L. Veisz, S. Karsch, F. Krausz, D. Habs, and J. Schreiber, *Phys. Rev. Lett.* **102**, 095002 (2009).
- [24] S. Kar, K. F. Kakolee, B. Qiao, A. Macchi, M. Cercez, D. Doria, M. Geissler, P. McKenna, D. Neely, J. Osterholz, R. Prasad, K. Quinn, B. Ramakrishna, G. Sarri, O. Willi, X. Y. Yuan, M. Zepf, and M. Borghesi, *Phys. Rev. Lett.* **109**, 185006 (2012).
- [25] A. Henig, S. Steinke, M. Schnürer, T. Sokollik, R. Hörlein, D. Kiefer, D. Jung, J. Schreiber, B. M. Hegelich, X. Q. Yan, J. Meyer-ter Vehn, T. Tajima, P. V. Nickles, W. Sandner, and D. Habs, *Phys. Rev. Lett.* **103**, 245003 (2009).
- [26] F. Dollar, C. Zülück, A. G. R. Thomas, V. Chvykov, J. Davis, G. Kalinchenko, T. Matsuoka, C. McGuffey, G. M. Petrov, L. Willingale, V. Yanovsky, A. Maksimchuk, and K. Krushelnick, *Phys. Rev. Lett.* **108**, 175005 (2012).
- [27] C. A. J. Palmer, J. Schreiber, S. R. Nagel, N. P. Dover, C. Bellei, F. N. Beg, S. Bott, R. J. Clarke, A. E. Dango, S. M. Hassan, P. Hilz, D. Jung, S. Kneip, S. P. D. Mangles, K. L. Lancaster, A. Rehman, A. P. L. Robinson, C. Spindloe, J. Szerypo, M. Tatarakis, M. Yeung, M. Zepf, and Z. Najmudin, *Phys. Rev. Lett.* **108**, 225002 (2012).
- [28] P. Kaw and J. Dawson, *Physics of Fluids (1958-1988)* **13**, 472 (1970).
- [29] S. Palaniyappan, B. M. Hegelich, H.-C. Wu, D. Jung, D. C. Gautier, L. Yin, B. J. Albright, R. P. Johnson, T. Shimada, S. Letzring, *et al.*, *Nature Physics* **8**, 763 (2012).
- [30] T. Grismayer, M. Vranic, J. L. Martins, R. Fonseca, and L. O. Silva, *Physical Review E* **95**, 023210 (2017).
- [31] T. Grismayer, M. Vranic, J. Martins, R. Fonseca, and L. Silva, *Phys. Plasmas* **23**, 056706 (2016).
- [32] T. Arber, K. Bennett, C. Brady, A. Lawrence-Douglas, M. Ramsay, N. Sircombe, P. Gillies, R. Evans, H. Schmitz, A. Bell, *et al.*, *Plasma Physics and Controlled Fusion* **57**, 113001 (2015).
- [33] W. Furry, *Physical Review* **81**, 115 (1951).
- [34] A. Di Piazza, C. Müller, K. Hatsagortsyan, and C. Keitel, *Reviews of Modern Physics* **84**, 1177 (2012).
- [35] C. Ridgers, J. G. Kirk, R. Ducloux, T. Blackburn, C. Brady, K. Bennett, T. Arber, and A. Bell, *Journal of Computational Physics* **260**, 273 (2014).
- [36] J. G. Kirk, A. Bell, and I. Arka, *Plasma Physics and Controlled Fusion* **51**, 085008 (2009).
- [37] C. Ridgers, C. S. Brady, R. Ducloux, J. Kirk, K. Bennett, T. Arber, A. Robinson, and A. Bell, *Phys. Rev. Lett.* **108**, 165006 (2012).
- [38] T. Schlegel, N. Naumova, V. Tikhonchuk, C. Labaune, I. Sokolov, and G. Mourou, *Phys. Plasmas* **16**, 083103 (2009).
- [39] A. Bashinov and A. Kim, *Physics of Plasmas* **20**, 113111 (2013).
- [40] L. Ji, A. Pukhov, E. Nerush, I. Y. Kostyukov, B. Shen, and K. Akli, *Physics of Plasmas* **21**, 023109 (2014).
- [41] C. S. Brady, C. Ridgers, T. Arber, A. Bell, and J. Kirk, *Phys. Rev. Lett.* **109**, 245006 (2012).
- [42] M. Levy, T. Blackburn, N. Ratan, J. Sadler, C. Ridgers, M. Kasim, L. Ceurvorst, J. Holloway, M. Baring, A. Bell, *et al.*, *arXiv preprint arXiv:1609.00389* (2016).
- [43] E. Nerush and I. Y. Kostyukov, *Plasma Physics and Controlled Fusion* **57**, 035007 (2015).
- [44] W. Heisenberg and H. Euler, *Zeitschrift für Physik* **98**, 714 (1936).
- [45] P. Zhang, C. Ridgers, and A. Thomas, *New Journal of Physics* **17**, 043051 (2015).